

There is more to quantum interferometry than entanglement

Thomas R. Bromley,^{1,*} Isabela A. Silva,^{1,2} Charlie O. Oncebay-Segura,²
Diogo O. Soares-Pinto,² Eduardo R. deAzevedo,² Tommaso Tufarelli,¹ and Gerardo Adesso¹

¹*Centre for the Mathematics and Theoretical Physics of Quantum Non-Equilibrium Systems,
School of Mathematical Sciences, The University of Nottingham, University Park, Nottingham NG7 2RD, UK*

²*Instituto de Física de São Carlos, Universidade de São Paulo,
P.O. Box 369, São Carlos, 13560-970 São Paulo, Brazil*

(Dated: November 23, 2024)

Entanglement has long stood as one of the characteristic features of quantum mechanics, yet recent developments have emphasized the importance of quantumness beyond entanglement for quantum foundations and technologies. We demonstrate that entanglement cannot entirely capture the worst-case sensitivity in quantum interferometry, when quantum probes are used to estimate the phase imprinted by a Hamiltonian, with fixed energy levels but variable eigenbasis, acting on one arm of an interferometer. This is shown by defining a bipartite entanglement monotone tailored to this interferometric setting and proving that it never exceeds the so-called interferometric power, a quantity which relies on more general quantum correlations beyond entanglement and captures the relevant resource. We then prove that the interferometric power can never increase when local commutativity preserving operations are applied to qubit probes, an important step to validate such a quantity as a genuine quantum correlations monotone. These findings are accompanied by a room temperature nuclear magnetic resonance experimental investigation, in which two-qubit states with extremal (maximal and minimal) interferometric power at fixed entanglement are produced and characterized.

I. INTRODUCTION

Entanglement is often perceived as the beating heart of quantum technologies [1–3]. It is the power behind a wealth of processes crucial for current innovations [4, 5], including quantum computing [6, 7] and cryptography [8]. Moreover, comprehending entanglement is of fundamental importance for quantum foundations [3], helping to demarcate the ever elusive boundary between classical physics and truly quantum phenomena [9, 10]. It is clear that what Schrödinger once termed *the* characteristic trait of quantum mechanics is central to our quantum journey [11]. However, the seemingly indisputable role of entanglement has been recently challenged by the idea of quantum correlations *beyond* entanglement [12–16]. These more general correlations, accounting for the inevitable disturbance caused by a local measurement on one subsystem of a genuinely quantum state, can play their own part in quantum enhanced processes, ranging from entanglement distribution to quantum state merging [15, 17–20].

Metrology, the science of high precision measurement, is one of the quintessential fields experiencing an advantage in the presence of entanglement: it has long been appreciated that measurements can be performed to greater precision by using an entangled collection of probes [21–24]. Despite this, the exact role of entanglement in the related task of quantum interferometry, which has far-reaching applications including gravitational wave detection [25], remains unclear [26]. The goal here is to precisely measure a phase shift φ by passing two quantum probes in a bipartite state ρ_{AB} through different arms of an interferometer [27, 28]. One arm actively imprints the phase φ onto probe A by a unitary transformation $U_A^\varphi = e^{-i\varphi H_A}$, generated by the Hamiltonian H_A , while

the other arm leaves probe B unchanged. An estimate $\tilde{\varphi}$ of the parameter is then constructed by carrying out suitable measurements on v copies of the output state of the probes $\rho_{AB}^\varphi = (U_A^\varphi \otimes \mathbb{I}_B)\rho_{AB}(U_A^\varphi \otimes \mathbb{I}_B)^\dagger$.

This estimate has an associated precision given by the mean squared error $\Delta^2 \tilde{\varphi}$, quantifying the statistical distance between $\tilde{\varphi}$ and φ . The objective is to reach the highest precision possible, but this is always limited by the Cramér-Rao bound $\Delta^2 \tilde{\varphi} \geq [\nu \mathcal{F}(\rho_{AB}, H_A)]^{-1}$ [29], with $\mathcal{F}(\rho_{AB}, H_A)$ the quantum Fisher information (QFI) [30, 31]. In the asymptotic limit $v \rightarrow \infty$, this bound can be saturated if optimal measurements are performed on the probes. The QFI thus stands as the relevant figure of merit in interferometry, capturing the sensitivity of ρ_{AB} to phase imprinting with a known Hamiltonian H_A .

A recent series of works [32–36] investigated the scenario where only the energy level spectrum Γ (assumed non-degenerate) of the Hamiltonian H_A is fixed a priori, while its eigenbasis is not known at the initial stage of preparation of the probe state, due e.g. to environmental fluctuations or set rules of a game. The family of possible Hamiltonians used to imprint the phase φ is then $H_A^\Gamma = V \text{diag}(\Gamma) V^\dagger$ for all unitaries V on subsystem A . In this setting, one is interested in gauging the usefulness of a given probe state ρ_{AB} for interferometry, regardless of the specific direction of phase imprinting. Such an analysis may lead to the identification of versatile probe states that can be useful as resources for precise phase estimation in several different bases. In particular, it becomes important to assess the *worst-case sensitivity*, obtained when H_A^Γ generates the nontrivial local dynamics (compliant with the fixed spectral constraint) to which the probe is the least sensitive. To test a probe state ρ_{AB} in such unfavourable conditions, an adversarial referee is assumed to operate the Hamiltonian H_A^Γ in a black box. The referee then reveals the selected eigenbasis only after the interaction, so that the most informative measurement given the prior preparation of ρ_{AB} and this posterior information on H_A^Γ can be performed on the output state ρ_{AB}^φ ,

* thomas.r.bromley@gmail.com

in order to estimate φ . Then, the relevant figure of merit for such a setup is the minimum QFI over all H_A^Γ , given by

$$\mathcal{P}_A^\Gamma(\rho_{AB}) = \frac{1}{4} \min_{H_A^\Gamma} \mathcal{F}(\rho_{AB}, H_A^\Gamma), \quad (1)$$

including a convenient normalization factor. This quantity, which captures the worst-case sensitivity to phase imprinting within the family of Hamiltonians H_A^Γ achievable by a probe state ρ_{AB} , has been aptly baptised *interferometric power* (IP) in [33]. Interestingly, the interferometric power vanishes if and only if ρ_{AB} is a *classical* state [32, 33] of the form

$$\rho_{AB} = \sum_i p_i |i\rangle\langle i|_A \otimes \rho_B^{(i)}, \quad (2)$$

with $\{|i\rangle_A\}$ any orthonormal basis of A and $\rho_B^{(i)}$ arbitrary states of B [15]. Notice that classical states of Eq. (2) form a strict subset of *separable* states, which in turn can be written as

$$\rho_{AB} = \sum_i p_i \rho_A^{(i)} \otimes \rho_B^{(i)}, \quad (3)$$

with $\rho_A^{(i)}$ arbitrary states of A . Therefore, the IP has been suggested as a quantifier of quantum correlations *beyond* entanglement in ρ_{AB} (with respect to probe A) [15, 33]. Operationally, a signature of these more general correlations is indeed the sensitivity to phase imprinting with all possible local Hamiltonian generators, that is, the ability to exhibit quantum coherence [37] in all possible local bases for probe A [15].

It is therefore natural to wonder where entanglement comes into play, if at all. In this paper, we shed light onto this question in quantitative terms by showing that entanglement, once suitably quantified, accounts only for a partial contribution to the available precision in quantum interferometry, hence formalizing a hierarchy of quantum resources useful for this task. In Section II we define a bipartite entanglement monotone, the *interferometric entanglement* (IE), specifically motivated from pure state interferometry, and show in Section III that it never exceeds the IP for arbitrary mixed bipartite quantum states. The IP is further proven in Section IV to never increase when qubit probes are subjected to local commutativity preserving operations [38–40], which constitute a meaningful set of free operations for the sought-after resource theory of quantum correlations [15]. This realizes an important progress towards establishing the IP as a fully fledged and operationally relevant quantum correlations monotone. In Section V we then investigate the relationship between IP and entanglement experimentally with a room temperature liquid-state nuclear magnetic resonance (NMR) implementation of a two-qubit system, in which case our IE reduces to the tangle (squared concurrence) [41–45] and the IP adopts a simple closed form [33]. Rank-2 states with the largest and smallest IP for a fixed tangle are generated and characterized, demonstrating that highly mixed states containing extremal quantum correlations additional to entanglement are accessible in laboratory, and could be adopted as robust probes for black box interferometry experiments [33]. We draw our concluding remarks in Section VI.

II. INTERFEROMETRIC ENTANGLEMENT

We define the IE for any pure bipartite probe state $|\psi\rangle_{AB}$ as

$$\mathcal{E}^\Gamma(|\psi\rangle_{AB}) = \min_{H_A^\Gamma} \mathcal{V}(|\psi\rangle_{AB}, H_A^\Gamma), \quad (4)$$

with the variance $\mathcal{V}(|\psi\rangle_{AB}, H_A^\Gamma) = {}_{AB}\langle\psi|(H_A^\Gamma)^2 \otimes \mathbb{I}_B |\psi\rangle_{AB} - ({}_{AB}\langle\psi| H_A^\Gamma \otimes \mathbb{I}_B |\psi\rangle_{AB})^2$. For pure states, the QFI reduces (up to a factor) to the variance, i.e. $\mathcal{F}(|\psi\rangle_{AB}, H_A^\Gamma) = 4\mathcal{V}(|\psi\rangle_{AB}, H_A^\Gamma)$ [23, 31], and so the IE is equal to the IP.

For a general mixed state ρ_{AB} , we use the standard convex roof construction to extend the definition of the IE as

$$\mathcal{E}^\Gamma(\rho_{AB}) = \min_{\{p_i, |\psi_i\rangle_{AB}\}} \sum_i p_i \mathcal{E}^\Gamma(|\psi_i\rangle_{AB}), \quad (5)$$

considering all decompositions of $\rho_{AB} = \sum_i p_i |\psi_i\rangle_{AB}\langle\psi_i|$ into pure states. We get that the IE is a full convex entanglement monotone, satisfying in particular the two key requirements stemming from the mathematical theory of entanglement as a resource [3, 46]: (i) $\mathcal{E}^\Gamma(\rho_{AB}) = 0$ for all separable states of Eq. (3); and (ii) $\mathcal{E}^\Gamma(\rho_{AB}) \geq \sum_i q_i \mathcal{E}^\Gamma(\rho_{AB}^{(i)})$ with $q_i = \text{Tr}(K_i \rho_{AB} K_i^\dagger)$ and $\rho_{AB}^{(i)} = K_i \rho_{AB} K_i^\dagger / q_i$, meaning that entanglement can never be generated or increased on average through local operations and classical communication (LOCC), where the product Kraus operators $\{K_i\}$ describe the action of a LOCC map, $\Lambda_{LOCC}(\rho_{AB}) = \sum_i K_i \rho_{AB} K_i^\dagger$. This holds by virtue of the convex roof extension [47], given that the quantity in Eq. (4) is a LOCC monotone for pure states [32]. Together with convexity, the properties above imply standard LOCC monotonicity for the IE, $\mathcal{E}^\Gamma(\rho_{AB}) \geq \mathcal{E}^\Gamma(\Lambda_{LOCC}(\rho_{AB}))$ [48].

III. HIERARCHY OF INTERFEROMETRIC FIGURES OF MERIT

The IE can be understood to quantify the worst-case sensitivity from the family of generating Hamiltonians H_A^Γ if one were to perform interferometry using individual pure probe states $|\psi_i\rangle_{AB}$ and then average the results with probabilities p_i . Conversely, the IP, as given by Eq. (1), represents the worst-case sensitivity by using the mixed state $\rho_{AB} = \sum_i p_i |\psi_i\rangle_{AB}\langle\psi_i|$ as a probe state directly. Furthermore, by virtue of the convex roof construction [49], the extension of the IE to mixed states in Eq. (5) amounts to the largest convex function which reduces to the worst-case sensitivity (that is, to the IP) for pure states. This indicates that both quantifiers are defined and physically motivated within the same operational setting, which makes their comparison meaningful.

Intuitively, one may then expect that the interferometric resource quantified by the IE can never exceed the figure of merit given by the IP, due to the extra minimization over all pure state decompositions of ρ_{AB} . We will now see that this intuition is true [50]. The first ingredient to use is that the QFI is (four times) the convex roof of the variance [51, 52],

$$\mathcal{F}(\rho_{AB}, H_A^\Gamma) = 4 \min_{\{p_i, |\psi_i\rangle\}} \sum_i p_i \mathcal{V}(|\psi_i\rangle_{AB}, H_A^\Gamma). \quad (6)$$

Using this fact, and the definition of the IE, we can say that

$$\begin{aligned}\mathcal{F}(\rho_{AB}, H_A^\Gamma) &= 4 \min_{\{\rho_i, |\psi_i\rangle\}} \sum_i p_i \mathcal{V}(|\psi_i\rangle_{AB}, H_A^\Gamma) \\ &\geq 4 \min_{\{\rho_i, |\psi_i\rangle\}} \sum_i p_i \min_{H_A^\Gamma} \mathcal{V}(|\psi_i\rangle_{AB}, H_A^\Gamma) \\ &= 4 \min_{\{\rho_i, |\psi_i\rangle\}} \sum_i p_i \mathcal{E}^\Gamma(|\psi_i\rangle_{AB}) \\ &= 4 \mathcal{E}^\Gamma(\rho_{AB}),\end{aligned}\quad (7)$$

where in the inequality we minimize over H_A^Γ , and in the second and third equalities we use the definition of IE in Eqs. (4) and (5). Finally, using the definition of IP in Eq. (1), we have

$$\mathcal{P}_A^\Gamma(\rho_{AB}) = \frac{1}{4} \min_{H_A^\Gamma} \mathcal{F}(\rho_{AB}, H_A^\Gamma) \geq \min_{H_A^\Gamma} \mathcal{E}^\Gamma(\rho_{AB}) = \mathcal{E}^\Gamma(\rho_{AB}). \quad (8)$$

We thus construct the fundamental hierarchy of resources:

$$\frac{1}{4} \mathcal{F}(\rho_{AB}, H_A^\Gamma) \geq \mathcal{P}_A^\Gamma(\rho_{AB}) \geq \mathcal{E}^\Gamma(\rho_{AB}), \quad \forall \rho_{AB}, H_A^\Gamma, \quad (9)$$

where the leftmost inequality holds by construction [33], while the rightmost inequality is our first main result. This shows that entanglement (quantified by IE) does not entirely capture the figure of merit in quantum interferometry, as it accounts only for a portion of the relevant quantum correlations (quantified by IP), which in turn provide a tighter lower bound to the QFI for any H_A^Γ . Note that any pure state saturates the rightmost inequality. Eq. (9) also succeeds in unifying different nonclassical signatures under the operational umbrella of interferometric phase estimation.

IV. INTERFEROMETRIC POWER AS A RESOURCE

In the following, we investigate the validation of the IP as a measure of quantum correlations beyond entanglement. In [33], the IP has been shown to obey the following properties: (a) $\mathcal{P}_A^\Gamma(\rho_{AB}) = 0$ iff ρ_{AB} is a classical state of the form Eq. (2); (b) $\mathcal{P}_A^\Gamma(\rho_{AB})$ is invariant under local unitaries; (c) $\mathcal{P}_A^\Gamma(\rho_{AB})$ reduces to an entanglement monotone for pure states (here identified as the IE); and (d) $\mathcal{P}_A^\Gamma(\rho_{AB})$ is non-increasing under the action of any local operation on subsystem B . These properties can be recognized as a set of necessary requirements for any good quantifier of quantum correlations [15, 32, 53, 54]. However, adopting a resource theory perspective [55–57] one should impose a more general monotonicity requirement, that any measure of our resource should not increase when a suitable set of free operations are applied to any state.

While LOCC are well established as the free operations for entanglement theory [3, 46], the corresponding set of free operations for more general quantum correlations has remained elusive. Recent findings have identified local commutativity preserving operations (LCPO) as the maximal set of local operations unable to create quantum correlations from an initial classical state [38–40]. The LCPO $\Lambda_{LCPO} = \Lambda_A \otimes \mathbb{I}_B$ preserve commutativity of local states on A , i.e. [50] $[\Lambda_A(\rho_A), \Lambda_A(\varsigma_A)] = 0 \quad \forall \rho_A, \varsigma_A$ such that $[\rho_A, \varsigma_A] = 0$. Monotonicity with respect to these operations has been proposed as

an additional requirement for any measure of quantum correlations [15], and so it is crucial to establish whether the IP has this property, i.e. if $\mathcal{P}_A^\Gamma(\rho_{AB}) \geq \mathcal{P}_A^\Gamma(\Lambda_{LCPO}(\rho_{AB}))$. We now prove that this is true when probe A is a qubit.

Restricted to qubits on A , the commutativity preserving operations are of two types, completely decohering and unital. The completely decohering operations map any state to one diagonal in a fixed reference basis $\{|i\rangle\}$, $\Lambda_A(\rho_A) = \sum_i p_i(\rho_A) |i\rangle\langle i|_A$, with $p_i(\rho_A)$ probabilities dependent on ρ_A , while unital operations preserve the identity, $\Lambda_A(\mathbb{I}_A) = \mathbb{I}_A$. Observing that local completely decohering operations Λ_A on A always return a classical state, i.e. $\Lambda_A(\rho_{AB})$ is of the form Eq. 2 for any input ρ_{AB} , it trivially follows that $\mathcal{P}_A^\Gamma(\rho_{AB}) \geq \mathcal{P}_A^\Gamma(\Lambda_A(\rho_{AB})) = 0$ in this case. We then need to show monotonicity of the IP under LCPO with unital operations Λ_A on A to guarantee overall monotonicity for qubit-qudit probes. The proof is provided in Appendix A.

When probe A has dimension $d_A > 2$, the commutativity preserving operations can be completely decohering (as above), or isotropic, $\Lambda_A(\rho_A) = t\Phi(\rho_A) + (1-t)\mathbb{I}_A/d_A$, where $\Phi(\rho_A)$ is either a unitary operation, i.e. $\Phi(\rho_A) = U_A \rho_A U_A^\dagger$ for some unitary U_A , or an antiunitary operation, i.e. $\Phi(\rho_A) = U_A \rho_A^T U_A^\dagger$ with ρ_A^T denoting the transpose of ρ_A . For $\Lambda_A(\rho_A)$ to be completely positive, t is constrained to $t \in [\frac{-1}{d_A^2-1}, 1]$ when Φ is unitary, and $t \in [\frac{-1}{d_A-1}, \frac{1}{d_A+1}]$ when Φ is antiunitary. We provide the operator-sum representation of $\Lambda_A(\rho_A)$ in Appendix B. Since again the completely decohering operations on A always return a classical state, investigating monotonicity of the IP under LCPO, when A is a qudit, requires testing monotonicity under isotropic operations Λ_A on A . In Appendix C, we prove such monotonicity when Φ is unitary and $t \in [0, 1]$, while the remaining cases are presently left as an open question. These results show that the IP is a full quantum correlations monotone for arbitrary qubit-qudit states, and a valid monotone under a subset of LCPO for general qudit-qudit states.

V. EXPERIMENTAL INVESTIGATION OF EXTREMAL STATES

We finally explore the interplay between IP and IE as captured by Eq. (9), via an in-depth numerical analysis supplemented by an experimental two-qubit NMR implementation using a BRUKER Ascend 600 MHz spectrometer at room temperature.

For two-qubit probes and a standard equispaced spectrum $\Gamma = \{-1, 1\}$ of our generating Hamiltonians H_A^Γ (we will drop the superscript Γ in what follows), the IE reduces to the tangle \mathcal{T} or squared concurrence [41–45], which is a monotonic function of the entanglement of formation (see Appendix D) while the IP \mathcal{P}_A also adopts a simple closed form [33]. Focussing on probes ρ_{AB} with rank-2 density matrices, we locate a family of states with the largest and smallest IP for a given tangle. This family is parameterized by two angles $\theta_1, \theta_2 \in [0, \pi/2]$, and can be expressed in the computational

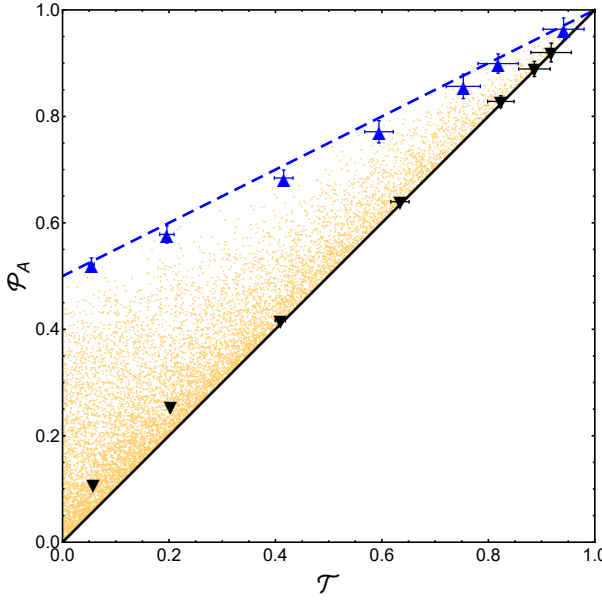


Figure 1. Comparison of the IP $\mathcal{P}_A(\rho_{AB})$ versus the IE, alias tangle $\mathcal{T}(\rho_{AB})$, for two-qubit rank-2 states ρ_{AB} . The lines correspond to the family of rank-2 X-states of Eq. (10) parameterized by θ_1 and θ_2 for two cases: (solid line) $\mathcal{P}_A(\rho_{AB}) = \mathcal{T}(\rho_{AB})$, which is the smallest IP for a given tangle; and (dashed line) $\mathcal{P}_A(\rho_{AB}) = \frac{1}{2}[1 + \mathcal{T}(\rho_{AB})]$, which is identified numerically as the largest IP for a given tangle amongst rank-2 states. The little squares depict 10^5 randomly generated rank-2 states, which are always found within the region given by $\mathcal{T}(\rho_{AB}) \leq \mathcal{P}_A(\rho_{AB}) \leq \frac{1}{2}[1 + \mathcal{T}(\rho_{AB})]$. The triangles correspond to experimental two-qubit states of the form Eq. (10) prepared using an NMR setup, with angles θ_1 and θ_2 given in Table I, to approach the lower extremal boundary (downward triangles) and the upper extremal one (upward triangles). Errors bars are calculated as detailed in the text.

basis as an X-state

$$\rho_{AB} = \frac{1}{2} \begin{pmatrix} c_+(\theta_1, \theta_2) & 0 & 0 & d_+(\theta_1, \theta_2) \\ 0 & s_+(\theta_1, \theta_2) & d_-(\theta_1, \theta_2) & 0 \\ 0 & d_-(\theta_1, \theta_2) & s_-(\theta_1, \theta_2) & 0 \\ d_+(\theta_1, \theta_2) & 0 & 0 & c_-(\theta_1, \theta_2) \end{pmatrix}, \quad (10)$$

with $c_{\pm}(\theta_1, \theta_2) = \cos^2\left(\frac{\theta_2}{2}\right)[1 \pm \sin(\theta_1)]$, $s_{\pm}(\theta_1, \theta_2) = \sin^2\left(\frac{\theta_2}{2}\right)[1 \pm \sin(\theta_1)]$, and $d_{\pm}(\theta_1, \theta_2) = -\frac{\cos(\theta_1)}{2}[1 \pm \cos(\theta_2)]$.

(i)	θ_2	$\pi/14$	$\pi/7$	$3\pi/14$	$2\pi/7$	$5\pi/14$	$3\pi/7$	$\pi/2$
(ii)	θ_1	0	$7\pi/90$	$\pi/9$	$13\pi/90$	$8\pi/45$	$19\pi/90$	$11\pi/45$
	θ_2	0	$\pi/10$	$\pi/10$	$7\pi/45$	$19\pi/90$	$3\pi/10$	$7\pi/18$

Table I. Values of θ_1 and θ_2 , applied with -x phase, for experimentally generated two-qubit states of Eq. (10), approximating (i) lower extremal states with IP equal to tangle ($\theta_1 = 0$), and (ii) upper extremal states with the largest IP for a given tangle amongst rank-2 states.

One may calculate the tangle and IP of ρ_{AB} to be

$$\mathcal{T}(\rho_{AB}) = \cos^2(\theta_1) \cos^2(\theta_2), \quad (11)$$

$$\mathcal{P}_A(\rho_{AB}) = \min \left\{ \cos(\theta_1)^2, \frac{3 - \cos(2\theta_1) + 2 \cos^2(\theta_1) \cos(2\theta_2)}{4} \right\}.$$

In particular, whenever $\theta_1 = 0$ we have that $\mathcal{P}_A(\rho_{AB}) = \mathcal{T}(\rho_{AB})$, identifying an extremal subset of rank-2 states for which the rightmost inequality in Eq. (9) is saturated (recall that this is also true for all pure, i.e. rank-1, states). Furthermore, when $\theta_1 = \arccos\left(\sqrt{\frac{1+T}{2}}\right)$ and $\theta_2 = \frac{1}{2} \arccos\left(3 - \frac{4}{1+T}\right)$ for some $T \in [0, 1]$, it holds that $\mathcal{T}(\rho_{AB}) = T$ and $\mathcal{P}_A(\rho_{AB}) = \frac{1}{2}[1 + \mathcal{T}(\rho_{AB})]$, which we conjecture to be the maximum IP for a given tangle that can be reached amongst all rank-2 states [58]. Fig. 1 plots the IP and tangle for these two cases. The conjecture is further supported by the numerical investigation of 10^5 rank-2 states randomly drawn from the uniform distribution according to the Hilbert-Schmidt measure [59], whose corresponding points in the IP vs tangle plane always lie in the triangular region between the two extremal cases, see Fig. 1.

In our experiment, the two-qubit system was encoded on ${}^1\text{H}$ and ${}^{13}\text{C}$ spin-1/2 nuclei in a Chloroform (CHCl_3) enriched with ${}^{13}\text{C}$ sample, allowing complete control of the amplitude and phase of each qubit separately [60–62]. Applying the pseudopure state technique [1, 63–66], the family of states in Eq. (10) can be implemented easily in our NMR setup by transformations in the deviation matrix of the thermal configuration. These states are obtained from the NMR radiofrequency pulse sequence described in Fig. 2, where the pseudopure state $|00\rangle\langle 00|$ is prepared as described in Ref. [66] (see Appendix E), and the quantum operations implemented by: $\text{cnot}-[\frac{\pi}{2}]_y^C \rightarrow U[\frac{1}{2}] \rightarrow [\frac{\pi}{2}]_x^C \rightarrow [\frac{\pi}{2}]_{-y}^C \rightarrow [\frac{\pi}{2}]_x^C \rightarrow [\frac{\pi}{2}]_y^C \rightarrow [\frac{\pi}{2}]_{-y}^H \rightarrow [\frac{\pi}{2}]_x^H \rightarrow [\frac{\pi}{2}]_y^H$ and $\text{HADAMARD}-[\frac{\pi}{2}]_y^H \rightarrow [\pi]_x^H$ [66]. In particular, states approximating the two extremal rank-2 classes with maximum and minimum IP for a given tangle were prepared by varying the angles θ_1 and θ_2 according to Table I. After state preparation, we performed a full 4-pulse quantum state tomography: $\mathbb{C}\mathbb{I}^H, [\frac{\pi}{2}]_x^C, [\frac{\pi}{2}]_y^C, [\frac{\pi}{2}]_x^H [\frac{\pi}{2}]_y^C$, as described in [67]. The resultant Uhlmann fidelity [68] with the corresponding target state was found always larger than 95%. Error bars were estimated by propagating the errors in pulse calibration (smaller than 3% per pulse, as determined by pulse width fitting) for the entire pulse sequence, and producing statistics based on one hundred computationally simulated runs per each preparation. Further experimental details are available in Appendix E.

VI. SUMMARY AND OUTLOOK

We reported results of fundamental and practical impact on the quantification of resources for quantum enhanced interferometry, advancing along three main paths.

First, we defined the IE, an entanglement monotone inspired by the figure of merit in interferometry, and shown that it can never exceed the IP, a quantifier of general quantum correlations introduced in [33]; this establishes a hierarchical relation between useful nonclassical resources, showing in par-

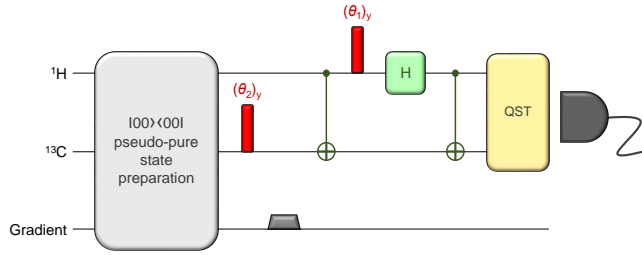


Figure 2. NMR pulse sequence to prepare two-qubit states of the form Eq. (10) using qubits encoded in ^1H and ^{13}C nuclear spins of Chloroform. Following state preparation as described in the text, we perform a 4-pulse quantum state tomography (QST) [67].

ticular the inability of entanglement to fully capture the precision available for estimating a phase φ imprinted by a Hamiltonian with a fixed spectrum but variable eigenbasis. We remark that this hierarchy exists specifically between IE and IP (which can be rightfully compared being derived from similar principles) and does not necessarily extend to other pairs of measures of entanglement and quantum correlations beyond entanglement. A worthwhile development will be to extend this analysis to other phase imprinting operations beside unitaries, such as noisy phase-covariant operations [36, 69], which are the free operations in a resource theory of quantum coherence viewed as asymmetry with respect to time translations [37, 70, 71].

Second, the *bona fide* role of the IP in quantum information theory has been further cemented by showing its monotonicity (for all qubit-qudit states) under LCPO, a postulated meaningful set of free operations for a resource theory of quantum correlations [15]. Further developments may identify a different set of free operations, possibly motivated from additional physical restrictions. However, since LCPO form the maximal set of local operations unable to create quantum correla-

tions [38–40], any such possible set of free operations must lie within LCPO and monotonicity of the IP will remain. Our next steps will be to investigate the full monotonicity of the IP under LCPO when operating locally on probes with dimension higher than two, which will be the focus of future work.

Third, we investigated how far quantum correlations can go *beyond* entanglement [72, 73] in two-qubit systems. We identified classes of extremal rank-2 states with maximum and minimum IP at given IE, and prepared instances of such states experimentally using a room temperature NMR setup. This shows that bipartite probe states offering substantial extra gain in performance for interferometry given a fixed degree of entanglement are accessible in laboratory. While maximum performance is always reached on pure maximally entangled states, finitely entangled states yet with extremal quantum correlations can be valuable whenever access to pure state preparations is precluded. It will be interesting to further explore the practical usefulness of quantum correlations beyond entanglement in technological settings such as quantum interferometry, metrology and discrimination [15, 26, 74], possibly with different experimental setups.

ACKNOWLEDGMENTS

This work was supported by the European Research Council (ERC) Starting Grant GQCOP (Grant No. 637352), the Foundational Questions Institute (fqxi.org) Physics of the Observer Programme (Grant No. FQXi-RFP-1601), the Royal Society International Exchanges (Grant No. IE150570) the CAPES Pesquisador Visitante Especial (Grant No. 108/2012), the CNPQ (Grant No. 312852/2014-2, 304955/2013-2, 443828/2014-8), and the Brazilian National Institute of Science and Technology of Quantum Information (INCT/IQ). E.R.d.A. thanks L. A. Colnago and Brazilian Agricultural Research Corporation (EMBRAPA Instrumentation) for NMR machine time. We thank K. Modi, G. Tóth, and S. Yu for helpful discussions.

- [1] M. A. Nielsen and I. L. Chuang, *Quantum computation and quantum information* (Cambridge University Press, Cambridge, 2010).
- [2] J. L. O’Brien, A. Furusawa, and J. Vučković, Nat. Photon. **3**, 687 (2009).
- [3] R. Horodecki, P. Horodecki, M. Horodecki, and K. Horodecki, Rev. Mod. Phys. **81**, 865 (2009).
- [4] V. Vedral, Nat. Phys. **10**, 256 (2014).
- [5] J. P. Dowling and G. J. Milburn, Phil. Trans. Roy. Soc. A **361**, 1655 (2003).
- [6] A. Steane, Rep. Prog. Phys. **61**, 117 (1998).
- [7] C. H. Bennett, E. Bernstein, G. Brassard, and U. Vazirani, SIAM journal on Computing **26**, 1510 (1997).
- [8] N. Gisin, G. Ribordy, W. Tittel, and H. Zbinden, Rev. Mod. Phys. **74**, 145 (2002).
- [9] S. Haroche and J. M. Raimond, *Exploring the quantum* (Oxford Univ. Press, 2006).
- [10] S. Haroche, Rev. Mod. Phys. **85**, 1083 (2013).
- [11] E. Schrödinger, in *Mathematical Proceedings of the Cambridge Philosophical Society*, Vol. 31 (Cambridge University Press, 1935) pp. 555–563.

- [12] H. Ollivier and W. H. Zurek, Phys. Rev. Lett. **88**, 017901 (2001).
- [13] L. Henderson and V. Vedral, J. Phys. A: Math. Gen. **34**, 6899 (2001).
- [14] K. Modi, A. Brodutch, H. Cable, T. Paterek, and V. Vedral, Rev. Mod. Phys. **84**, 1655 (2012).
- [15] G. Adesso, T. R. Bromley, and M. Cianciaruso, J. Phys. A: Math. Theor. **49**, 473001 (2016).
- [16] G. Adesso, M. Cianciaruso, and T. R. Bromley, arXiv preprint arXiv:1611.01959 (2016).
- [17] T. Chuan, J. Maillard, K. Modi, T. Paterek, M. Paternostro, and M. Piani, Phys. Rev. Lett. **109**, 070501 (2012).
- [18] A. Streltsov, H. Kampermann, and D. Bruß, Phys. Rev. Lett. **108**, 250501 (2012).
- [19] D. Cavalcanti, L. Aolita, S. Boixo, K. Modi, M. Piani, and A. Winter, Phys. Rev. A **83**, 032324 (2011).
- [20] V. Madhok and A. Datta, Phys. Rev. A **83**, 032323 (2011).

- [21] V. Giovannetti, S. Lloyd, and L. Maccone, Phys. Rev. Lett. **96**, 010401 (2006).
- [22] V. Giovannetti, S. Lloyd, and L. Maccone, Nat. Photon. **5**, 222 (2011).
- [23] G. Tóth and I. Apellaniz, J. Phys. A: Math. Theor. **47**, 424006 (2014).
- [24] L. Pezzé, A. Smerzi, M. K. Oberthaler, R. Schmied, and P. Treutlein, arXiv preprint arXiv:1609.01609 (2016).
- [25] B P. Abbott *et al.* (LIGO Scientific Collaboration and Virgo Collaboration), Phys. Rev. Lett. **116**, 061102 (2016).
- [26] D. Braun, G. Adesso, F. Benatti, R. Floreanini, U. Marzolini, M. W. Mitchell, and S. Pirandola, arXiv preprint arXiv:1701.05152 (2017).
- [27] C. M. Caves, Phys. Rev. D **23**, 1693 (1981).
- [28] R. Demkowicz-Dobrzański, M. Jarzyna, and J. Kolodyński (Elsevier, 2015) pp. 345 – 435.
- [29] C. W. Helstrom, *Quantum detection and estimation theory*, Vol. 123 (Academic press, 1976).
- [30] S. L. Braunstein and C. M. Caves, Phys. Rev. Lett. **72**, 3439 (1994).
- [31] M. G. Paris, Int. J. Quant. Inf. **7**, 125 (2009).
- [32] D. Girolami, T. Tufarelli, and G. Adesso, Phys. Rev. Lett. **110**, 240402 (2013).
- [33] D. Girolami, A. M. Souza, V. Giovannetti, T. Tufarelli, J. G. Filgueiras, R. S. Sarthour, D. O. Soares-Pinto, I. S. Oliveira, and G. Adesso, Phys. Rev. Lett. **112**, 210401 (2014).
- [34] G. Adesso, Phys. Rev. A **90**, 022321 (2014).
- [35] A. Farace, A. De Pasquale, G. Adesso, and V. Giovannetti, New J. Phys. **18**, 013049 (2016).
- [36] R. Nichols, T. R. Bromley, L. A. Correa, and G. Adesso, Phys. Rev. A **94**, 042101 (2016).
- [37] A. Streltsov, G. Adesso, and M. B. Plenio, arXiv preprint arXiv:1609.02439 (2016).
- [38] X. Hu, H. Fan, D. Zhou, and W.-M. Liu, Phys. Rev. A **85**, 032102 (2012).
- [39] Y. Guo and J. Hou, J. Phys. A: Math. Theor. **46**, 155301 (2013).
- [40] A. Streltsov, H. Kampermann, and D. Bruß, Phys. Rev. Lett. **107**, 170502 (2011).
- [41] V. Coffman, J. Kundu, and W. K. Wootters, Phys. Rev. A **61**, 052306 (2000).
- [42] S. Hill and W. K. Wootters, Phys. Rev. Lett. **78**, 5022 (1997).
- [43] W. K. Wootters, Phys. Rev. Lett. **80**, 2245 (1998).
- [44] P. Rungta, V. Bužek, C. M. Caves, M. Hillery, and G. J. Milburn, Phys. Rev. A **64**, 042315 (2001).
- [45] P. Rungta and C. M. Caves, Phys. Rev. A **67**, 012307 (2003).
- [46] M. B. Plenio and S. Virmani, Quantum Inf. Comput. **7**, 1 (2007).
- [47] G. Vidal, J. Mod. Opt. **47**, 355 (2000).
- [48] V. Vedral and M. B. Plenio, Phys. Rev. A **57**, 1619 (1998).
- [49] A. Uhlmann, Entropy **12**, 1799 (2010).
- [50] Note however that such a hierarchy is non-trivial and does not hold generally for a pair of quantifiers of entanglement and quantum correlations beyond entanglement, even if defined by similar methods as the two quantities considered here. For instance, in quantum information theory, two of the most common measures of entanglement and general quantum correlations are the entanglement of formation $E^f(\rho_{AB})$ and the quantum discord $D_A(\rho_{AB})$, respectively [12, 15, 46]. These two measures coincide on pure states (reducing to the entropy of entanglement), while the entanglement of formation is extended to mixed states via the convex roof construction. However, there is no strict inequality between them, $E^f(\rho_{AB}) \leq D_A(\rho_{AB})$, meaning that one quantity may be larger or smaller than the other depending on the state ρ_{AB} [14]. On the other hand, Eq. (8) shows that inter-
- ferometrically inspired measures of entanglement and quantum correlations beyond entanglement do obey a strict inequality, $E^f(\rho_{AB}) \leq \mathcal{P}_A^f(\rho_{AB})$, for any state ρ_{AB} .
- [51] G. Tóth and D. Petz, Phys. Rev. A **87**, 032324 (2013).
- [52] S. Yu, arXiv preprint arXiv:1302.5311 (2013).
- [53] A. Streltsov, H. Kampermann, and D. Bruß, Phys. Rev. Lett. **106**, 160401 (2011).
- [54] B. Aaronson, R. L. Franco, and G. Adesso, Phys. Rev. A **88**, 012120 (2013).
- [55] M. Horodecki and J. Oppenheim, Int. J. Mod. Phys. B **27**, 1345019 (2013).
- [56] B. Coecke, T. Fritz, and R. W. Spekkens, Information and Computation **250**, 59 (2016).
- [57] F. G. S. L. Brandão, M. Horodecki, N. Ng, J. Oppenheim, and S. Wehner, Proc. Natl. Acad. Sci. **112**, 3275 (2015).
- [58] By using Lagrange multipliers, one can prove rigorously that such states maximize the IP at given tangle amongst all two-qubit X-states of rank 2. However, instances of states with rank 3 and 4 can be found with even larger IP at fixed nonzero tangle.
- [59] I. Bengtsson and K. Zyczkowski, *Geometry of quantum states: an introduction to quantum entanglement* (Cambridge University Press, 2007).
- [60] I. A. Silva, D. Girolami, R. Accaise, R. S. Sarthour, I. S. Oliveira, T. J. Bonagamba, E. R. deAzevedo, D. O. Soares-Pinto, and G. Adesso, Phys. Rev. Lett. **110**, 140501 (2013).
- [61] F. M. Paula, I. A. Silva, J. D. Montealegre, A. M. Souza, E. R. deAzevedo, R. S. Sarthour, A. Saguia, I. S. Oliveira, D. O. Soares-Pinto, G. Adesso, and M. S. Sarandy, Phys. Rev. Lett. **111**, 250401 (2013).
- [62] I. A. Silva, A. M. Souza, T. R. Bromley, M. Cianciaruso, R. Marx, R. S. Sarthour, I. S. Oliveira, R. Lo Franco, S. J. Glaser, E. R. deAzevedo, D. O. Soares-Pinto, and G. Adesso, Phys. Rev. Lett. **117**, 160402 (2016).
- [63] N. A. Gershenfeld and I. L. Chuang, Science **275**, 350 (1997).
- [64] D. G. Cory, A. F. Fahmy, and T. F. Havel, Proc. Natl. Acad. Sci. **94**, 1634 (1997).
- [65] E. Knill, I. Chuang, and R. Laflamme, Phys. Rev. A **57**, 3348 (1998).
- [66] I. Oliveira, R. Sarthour Jr, T. Bonagamba, E. Azevedo, and J. C. Freitas, *NMR quantum information processing* (Elsevier, 2011).
- [67] G. Long, H. Yan, and Y. Sun, J. Opt. B: Quant. Semiclass. Opt. **3**, 376 (2001).
- [68] A. Uhlmann, Rep. Math. Phys. **9**, 273 (1976).
- [69] A. Smirne, J. Kołodyński, S. F. Huelga, and R. Demkowicz-Dobrzański, Phys. Rev. Lett. **116**, 120801 (2016).
- [70] I. Marvian and R. W. Spekkens, Nat. Commun. **5** (2014).
- [71] I. Marvian, R. W. Spekkens, and P. Zanardi, Phys. Rev. A **93**, 052331 (2016).
- [72] D. Girolami and G. Adesso, Phys. Rev. A **84**, 052110 (2011).
- [73] M. Piani and G. Adesso, Phys. Rev. A **85**, 040301 (2012).
- [74] P. Bogaert and D. Girolami, arXiv preprint arXiv:1609.02170 (2016).
- [75] M. Keyl, Phys. Rep. **369**, 431 (2002).
- [76] C. B. Mendl and M. M. Wolf, Comm. Math. Phys. **289**, 1057 (2009).
- [77] R. A. Bertlmann and P. Krammer, J. Phys. A: Math. Theor. **41**, 235303 (2008).

Appendix A: Monotonicity of the IP under local unital maps for qubit-qudit systems

We will prove that $\mathcal{P}_A^\Gamma(\rho_{AB}) \geq \mathcal{P}_A^\Gamma(\Lambda_A \otimes \mathbb{I}_B(\rho_{AB}))$ for qubit-qudit states ρ_{AB} and unital operations Λ_A acting on A , i.e. where Λ_A preserves the identity. Consider the dilation τ_{ABC} of $\Lambda_A \otimes \mathbb{I}_B(\rho_{AB})$ into a larger space including an extra ancillary system C , such that $\text{Tr}_C[\tau_{ABC}] = \Lambda_A \otimes \mathbb{I}_B(\rho_{AB})$ [75]. The following inequality holds

$$\mathcal{P}_A^\Gamma(\tau_{ABC}) \geq \mathcal{P}_A^\Gamma(\text{Tr}_C[\tau_{ABC}]) = \mathcal{P}_A^\Gamma(\Lambda_A \otimes \mathbb{I}_B(\rho_{AB})), \quad (\text{A1})$$

since the IP never increases under any operation on subsystems other than A [33]. It is then sufficient to prove that $\mathcal{P}_A^\Gamma(\rho_{AB}) \geq \mathcal{P}_A^\Gamma(\tau_{ABC})$ to arrive at the desired inequality. To do this, we use the fact that any unital qubit operation can be equivalently written as a convex combination of unitaries (or random unitary channel) [76], i.e.

$$\Lambda_A(\rho_A) = \sum_i p_i U_A^{(i)} \rho_A (U_A^{(i)})^\dagger \quad (\text{A2})$$

for some mixture of unitaries $\{U_A^{(i)}\}$ with probabilities $\{p_i\}$ acting on subsystem A in the state ρ_A . This can be used to explicitly write the diluted state as

$$\tau_{ABC} = U_{ABC}(\rho_{AB} \otimes |\alpha\rangle\langle\alpha|_C)U_{ABC}^\dagger, \quad (\text{A3})$$

We can then write

$$\begin{aligned} M' &= \frac{1}{2} \sum_{mn} \frac{(q_m - q_n)^2}{q_m + q_n} \langle \Phi_m | \vec{\sigma}_A \otimes \mathbb{I}_{BC} | \Phi_n \rangle \langle \Phi_n | \vec{\sigma}_A^T \otimes \mathbb{I}_{BC} | \Phi_m \rangle \\ &= \frac{1}{2} \sum_{mn} \frac{(q_m - q_n)^2}{q_m + q_n} \langle \phi_m |_{AB} \otimes \langle \alpha |_C U_{ABC}^\dagger \vec{\sigma}_A \otimes \mathbb{I}_{BC} U_{ABC} | \phi_n \rangle_{AB} \otimes |\alpha\rangle_C \langle \phi_n |_{AB} \otimes \langle \alpha |_C U_{ABC}^\dagger \vec{\sigma}_A^T \otimes \mathbb{I}_{BC} U_{ABC} | \phi_m \rangle_{AB} \otimes |\alpha\rangle_C \\ &= \frac{1}{2} \sum_{mn} \frac{(q_m - q_n)^2}{q_m + q_n} \langle \phi_m | \sum_i p_i (U_A^{(i)})^\dagger \vec{\sigma}_A U_A^{(i)} \otimes \mathbb{I}_B | \phi_n \rangle \langle \phi_n | \sum_j p_j (U_A^{(j)})^\dagger \vec{\sigma}_A^T U_A^{(j)} \otimes \mathbb{I}_B | \phi_m \rangle, \end{aligned} \quad (\text{A7})$$

where we have used the fact that $U_{ABC} |\alpha\rangle_C = \sum_i \sqrt{p_i} U_A^{(i)} \otimes \mathbb{I}_B |i\rangle_C$. From the well known correspondence between the special unitary group $SU(2)$ and special orthogonal group $SO(3)$, we can see that for each i there exists an orthogonal matrix R_i such that $(U_A^{(i)})^\dagger \vec{\sigma}_A U_A^{(i)} = R_i \vec{\sigma}_A$. We thus obtain

$$M' = LML^T, \quad (\text{A8})$$

where $L = \sum_i p_i R_i$ is a real matrix such that $L^T L \leq \mathbb{I}$.

Finally, let us consider the eigenvalues of M' . If L is non-invertible we know that M' has a zero eigenvalue, and hence $\mathcal{P}_A^\Gamma(\rho_{AB}) \geq \mathcal{P}_A^\Gamma(\tau_{ABC}) = 0$. Instead, if M' is invertible, consider the unit vector $|v\rangle$ constructed by

$$|v\rangle = \frac{(L^T)^{-1} |v\rangle_0}{\|(L^T)^{-1} |v\rangle_0\|}, \quad (\text{A9})$$

where $|v\rangle_0$ is the eigenvector of M corresponding to the smallest eigenvalue $\lambda_{\min} \equiv \min\{\lambda_i\}$ of M . It is then simple to see

with

$$\begin{aligned} U_{ABC} &= \sum_i U_A^{(i)} \otimes \mathbb{I}_B \otimes |i\rangle\langle i|_C, \\ |\alpha\rangle_C &= \sum_i \sqrt{p_i} |i\rangle_C. \end{aligned} \quad (\text{A4})$$

We now make use of the explicit form of the IP for qubit-qudit states given in [33], $\mathcal{P}_A^\Gamma(\rho_{AB}) = \alpha^2 \min\{\lambda_i\}$, where $\{\lambda_i\}$ are the eigenvalues of the 3×3 matrix

$$M = \frac{1}{2} \sum_{m,n:q_m+q_n \neq 0} \frac{(q_m - q_n)^2}{q_m + q_n} \langle \phi_m | \vec{\sigma}_A \otimes \mathbb{I}_B | \phi_n \rangle \langle \phi_n | \vec{\sigma}_A^T \otimes \mathbb{I}_B | \phi_m \rangle, \quad (\text{A5})$$

with q_m and $|\phi_m\rangle_{AB}$ the eigenvalues and normalised eigenvectors of ρ_{AB} , and $\vec{\sigma}_A$ the vector of the three Pauli matrices. We write any two-level spectrum as $\Gamma = \{\beta - \alpha, \beta + \alpha\}$ with $\alpha, \beta \in \mathbb{R}$. For convenience, in the following we set $\alpha = 1$ and $\beta = 0$ and consider the standard equispaced spectrum $\{-1, 1\}$, but the proof holds for any α and β . The task is then to calculate the matrix M' corresponding to τ_{ABC} . The eigenvalues of τ_{ABC} are the same as those of ρ_{AB} , while the eigenvectors are given by

$$|\Phi_m\rangle_{ABC} = U_{ABC} |\phi_m\rangle_{AB} \otimes |\alpha\rangle_C. \quad (\text{A6})$$

that

$$\lambda'_{\min} \leq \langle v | M' | v \rangle = \frac{\lambda_{\min}}{\|(L^T)^{-1} |v\rangle_0\|^2} \leq \lambda_{\min}, \quad (\text{A10})$$

where λ'_{\min} is the minimum eigenvalue of M' and we have used the fact that $\|(L^T)^{-1} |v\rangle_0\| \geq 1$ since $L^T L \leq \mathbb{I}$. Combined with Eq. (A1), we then have that

$$\mathcal{P}_A^\Gamma(\rho_{AB}) = \lambda_{\min} \geq \lambda'_{\min} = \mathcal{P}_A^\Gamma(\tau_{ABC}) \geq \mathcal{P}_A^\Gamma(\Lambda_A \otimes \mathbb{I}_B(\rho_{AB})), \quad (\text{A11})$$

establishing the monotonicity of the IP under qubit unital operations on probe A .

Appendix B: Operator-sum representation of isotropic operations

Here we provide explicitly the Kraus decomposition of the isotropic operations [38]

$$\Lambda_A(\rho_A) = t\Phi(\rho_A) + (1-t)\frac{\mathbb{I}_A}{d}, \quad (\text{B1})$$

for the two cases of unitary Φ and antiunitary Φ , d being the dimension of system A . In particular, we shall provide the Kraus decomposition when $U_A = \mathbb{I}_A$. To find the Kraus decomposition for a general U_A , one simply needs to transform the following Kraus operators by $K_i \rightarrow U_A K_i$. Note that quantum correlations are invariant under local unitary transformations U_A , and so for our purposes it is sufficient to treat only the case $U_A = \mathbb{I}_A$.

Let us denote by $\{K_i\}$ the Kraus operators for the operator-sum representation of Λ_A ,

$$\Lambda_A(X) = \sum_i K_i X K_i^\dagger, \quad (\text{B2})$$

where the condition $\sum_i K_i^\dagger K_i = \mathbb{I}_A$ must be satisfied for Λ_A to be completely positive and trace preserving. In the following we shall first determine the allowed range of the parameter t for both the unitary and antiunitary case, by imposing positivity of the Choi state. We introduce an ancilla A' which is a copy of A ; for brevity we shall indicate the computational basis of the joint AA' system as $|k, l\rangle \equiv |k\rangle_A \otimes |l\rangle_{A'}$. The Choi state is then given by

$$\tau = \Lambda_A \otimes \mathcal{I}_{A'}(|\Psi_+\rangle\langle\Psi_+|) \quad (\text{B3})$$

where $|\Psi_+\rangle = \frac{1}{\sqrt{d}} \sum_{k=0}^{d-1} |k, k\rangle$ and \mathcal{I} indicates the identity superoperator. Having imposed $\tau \geq 0$, we will then report the Kraus operators of Λ_A and verify their completeness.

1. Unitary case

First we consider the unitary Φ case. We only need concern ourselves with maps featuring $U_A = \mathbb{I}_A$. For any bipartite state $\rho_{AA'}$ we thus have $\Lambda_A \otimes \mathcal{I}_{A'}(\rho_{AA'}) = t\rho_{AA'} + (1-t)\frac{\mathbb{I}_A}{d} \otimes \text{Tr}_A(\rho_{AA'})$. The corresponding Choi state reads

$$\tau = t|\Psi_+\rangle\langle\Psi_+| + \frac{1-t}{d^2}\mathbb{I}_A \otimes \mathbb{I}_{A'}. \quad (\text{B4})$$

From the above we easily conclude that the spectrum of τ is $\{t+(1-t)/d^2, (1-t)/d^2\}$. Imposing the latter to be non-negative we obtain the allowed range

$$-\frac{1}{d^2-1} \leq t \leq 1, \quad (\text{B5})$$

which is tighter than what was reported in [38]. We shall now provide an explicit Kraus representation of the map. Consider the $d^2 - 1$ generalized Pauli matrices $\{\gamma_i\}_{i=1}^{d^2-1}$ [77], and fix the

d -dimensional identity matrix as $\gamma_0 = \mathbb{I}_A$. The d^2 Kraus operators $\{K_i\}_{i=0}^{d^2-1}$ are then

$$K_0 = \sqrt{\frac{1 + (d^2 - 1)t}{d^2}}\gamma_0, \\ K_i = \sqrt{\frac{1-t}{2d}}\gamma_i \quad \forall i \in \{1, 2, \dots, d^2 - 1\}. \quad (\text{B6})$$

We can now verify the condition $\sum_{i=0}^{d^2-1} K_i^\dagger K_i = \mathbb{I}_A$. Since the Kraus operators are Hermitian, and since $\gamma_0^2 = \mathbb{I}_A$ and $\sum_{i=1}^{d^2-1} \gamma_i^2 = \frac{2(d^2-1)}{d}\mathbb{I}_A$, we have

$$\begin{aligned} \sum_{i=0}^{d^2-1} K_i^\dagger K_i &= \left(\left| \frac{1 + (d^2 - 1)t}{d^2} \right| + \frac{2(d^2 - 1)}{d} \times \left| \frac{1-t}{2d} \right| \right) \mathbb{I}_A \\ &= \frac{1}{d^2} (|1 + (d^2 - 1)t| + (d^2 - 1)|1-t|) \mathbb{I}_A. \end{aligned} \quad (\text{B7})$$

Exploiting Eq. (B5) we may simplify $|1 + (d^2 - 1)t| = 1 + (d^2 - 1)t$ and $|1-t| = 1-t$, hence

$$\begin{aligned} \sum_{i=0}^{d^2-1} K_i^\dagger K_i &= \frac{1}{d^2} (1 + (d^2 - 1)t + (d^2 - 1)(1-t)) \mathbb{I}_A \\ &= \mathbb{I}_A. \end{aligned} \quad (\text{B8})$$

2. Antiunitary case

Now we treat the more complicated case of Φ being antiunitary (again, fixing $U_A = \mathbb{I}_A$). We thus have $\Lambda_A \otimes \mathcal{I}_{A'}(\rho_{AA'}) = t\rho_{AA'}^{T_A} + (1-t)\frac{\mathbb{I}_A}{d} \otimes \text{Tr}_A(\rho_{AA'})$, where T_A indicates partial transposition on system A . The corresponding Choi state reads

$$\tau = \frac{t}{d} \sum_{k,l=0}^{d-1} |k, l\rangle\langle l, k| + \frac{1-t}{d^2} \mathbb{I}_A \otimes \mathbb{I}_{A'}. \quad (\text{B9})$$

By inspection we find that the eigenvectors of τ are in this case $|k, k\rangle$ with $k = 0, \dots, d-1$, and $\frac{1}{\sqrt{2}}(|k, l\rangle \pm |l, k\rangle)$ for all pairs $k < l$. The spectrum of τ is then $\{(1-t)/d^2, t/d + (1-t)/d^2, -t/d + (1-t)/d^2\}$, from which we derive the constraint

$$-\frac{1}{d-1} \leq t \leq \frac{1}{d+1}. \quad (\text{B10})$$

As before, to write down a Kraus decomposition we can use the generalized Pauli matrices $\{\gamma_i\}_{i=1}^{d^2-1}$ with the identity $\gamma_0 = \mathbb{I}_A$. Now, consider the set of vectorizations of the generalized Pauli matrices, $\{\vec{\gamma}_i\}_{i=1}^{d^2-1}$ with $\vec{\gamma}_i = \text{vec}(\gamma_i)$, where $\text{vec}(X) = (\langle 0|X|0\rangle, \langle 0|X|1\rangle, \dots, \langle 0|X|d\rangle, \langle 1|X|0\rangle, \langle 1|X|1\rangle, \dots, \langle d|X|d\rangle)$ is the vectorization of a matrix. We can split the generalized Pauli matrices into two categories based on their corresponding vectorizations: (1) $\text{sign}(\vec{\gamma}_i \cdot \vec{\gamma}_i) = 1$, and (2) $\text{sign}(\vec{\gamma}_i \cdot \vec{\gamma}_i) = -1$. There are $(d+2)(d-1)/2$ generalized Pauli matrices of type (1) and $d(d-1)/2$ of type (2), and we call the generalized Pauli matrices of type (1): $\{\gamma_i^{(1)}\}_{i=1}^{(d+2)(d-1)/2}$,

and of type (2): $\{\gamma_i^{(2)}\}_{i=1}^{d(d-1)/2}$. Now we can give the Kraus decomposition

$$\begin{aligned} K_0 &= \sqrt{\frac{1 + (d - 1)t}{d^2}} \gamma_0, \\ K_i &= \sqrt{\frac{1 + (d - 1)t}{2d}} \gamma_i^{(1)} \quad \forall i \in \{1, 2, \dots, \frac{(d+2)(d-1)}{2}\}, \\ K_{i+\frac{(d+2)(d-1)}{2}} &= \sqrt{\frac{1 - (d + 1)t}{2d}} \gamma_i^{(2)} \quad \forall i \in \{1, 2, \dots, \frac{d(d-1)}{2}\}. \end{aligned} \quad (\text{B11})$$

We can also consider the condition $\sum_{i=0}^{d^2-1} K_i^\dagger K_i = \mathbb{I}_A$. Since the Kraus operators are Hermitian, and since $\gamma_0^2 = \mathbb{I}_A$, $\sum_{i=1}^{(d+2)(d-1)/2} (\gamma_i^{(1)})^2 = \frac{d^2+d-2}{d} \mathbb{I}_A$ and $\sum_{i=1}^{d(d-1)/2} (\gamma_i^{(2)})^2 = (d - 1) \mathbb{I}_A$, we have

$$\begin{aligned} \sum_{i=0}^{d^2-1} K_i^\dagger K_i &= \left(\left| \frac{1 + (d - 1)t}{d^2} \right| + \frac{d^2 + d - 2}{d} \times \left| \frac{1 + (d - 1)t}{2d} \right| \right. \\ &\quad \left. + (d - 1) \left| \frac{1 - (d + 1)t}{2d} \right| \right) \mathbb{I}_A \\ &= \frac{1}{d^2} \left(|1 + (d - 1)t| + \frac{(d^2 + d - 2)}{2} |1 + (d - 1)t| \right. \\ &\quad \left. + \frac{d^2 - d}{2} |1 - (d + 1)t| \right) \mathbb{I}_A \\ &= \frac{1}{2d^2} ((d^2 + d) |1 + (d - 1)t| + (d^2 - d) |1 - (d + 1)t|). \end{aligned}$$

Then, we may use Eq. (B10) to simplify $|1 + (d - 1)t| = 1 + (d - 1)t$ and $|1 - (d + 1)t| = 1 - (d + 1)t$, yielding $\sum_{i=0}^{d^2-1} K_i^\dagger K_i = \mathbb{I}_A$.

Appendix C: Monotonicity of the IP under unitary isotropic operations

We now will prove that $\mathcal{P}_A^\Gamma(\rho_{AB}) \geq \mathcal{P}_A^\Gamma(\Lambda_A \otimes \mathbb{I}_B(\rho_{AB}))$ when A has dimension larger than 2 and for isotropic operations with unitary Φ and $t \in [0, 1]$. For this range of t , we have that $\Lambda_A \otimes \mathbb{I}_B(\rho_{AB})$ is just a convex combination between $U_A \otimes \mathbb{I}_B \rho_{AB} U_A^\dagger \otimes \mathbb{I}_B$ and $\mathbb{I}_A/d_A \otimes \text{Tr}_A(\rho_{AB})$. From convexity of the QFI [52] it holds that

$$\begin{aligned} &\mathcal{F}(\Lambda_A \otimes \mathbb{I}_B(\rho_{AB}), H_A^\Gamma \otimes \mathbb{I}_B) \\ &= \mathcal{F}\left(t U_A \otimes \mathbb{I}_B \rho_{AB} U_A^\dagger \otimes \mathbb{I}_B + (1 - t) \frac{\mathbb{I}_A}{d_A} \otimes \text{Tr}_A(\rho_{AB}), H_A^\Gamma \otimes \mathbb{I}_B\right) \\ &\leq t \mathcal{F}(U_A \otimes \mathbb{I}_B \rho_{AB} U_A^\dagger \otimes \mathbb{I}_B, H_A^\Gamma \otimes \mathbb{I}_B) \\ &\quad + (1 - t) \mathcal{F}\left(\frac{\mathbb{I}_A}{d_A} \otimes \text{Tr}_A(\rho_{AB}), H_A^\Gamma \otimes \mathbb{I}_B\right) \\ &= t \mathcal{F}(U_A \otimes \mathbb{I}_B \rho_{AB} U_A^\dagger \otimes \mathbb{I}_B, H_A^\Gamma \otimes \mathbb{I}_B) \\ &\leq \mathcal{F}(U_A \otimes \mathbb{I}_B \rho_{AB} U_A^\dagger \otimes \mathbb{I}_B, H_A^\Gamma \otimes \mathbb{I}_B), \end{aligned} \quad (\text{C1})$$

where in the second equality we use the fact that $\mathcal{F}\left(\frac{\mathbb{I}_A}{d_A} \otimes \text{Tr}_A(\rho_{AB}), H_A^\Gamma \otimes \mathbb{I}_B\right) = 0$, which follows by noting that

$\left[\frac{\mathbb{I}_A}{d_A} \otimes \text{Tr}_A(\rho_{AB}), H_A^\Gamma \otimes \mathbb{I}_B \right] = 0$. Using the above inequality, we arrive at the monotonicity of the IP,

$$\begin{aligned} \mathcal{P}_A^\Gamma(\Lambda_A \otimes \mathbb{I}_B(\rho_{AB})) &= \frac{1}{4} \min_{H_A^\Gamma} \mathcal{F}(\Lambda_A \otimes \mathbb{I}_B(\rho_{AB}), H_A^\Gamma \otimes \mathbb{I}_B) \\ &\leq \frac{1}{4} \min_{H_A^\Gamma} \mathcal{F}(U_A \otimes \mathbb{I}_B \rho_{AB} U_A^\dagger \otimes \mathbb{I}_B, H_A^\Gamma \otimes \mathbb{I}_B) \\ &= \mathcal{P}_A^\Gamma(U_A \otimes \mathbb{I}_B \rho_{AB} U_A^\dagger \otimes \mathbb{I}_B) \\ &= \mathcal{P}_A^\Gamma(\rho_{AB}), \end{aligned} \quad (\text{C2})$$

where in the third equality we use the invariance of the IP under local unitary transformations.

Appendix D: Equivalence between the IE and the I-tangle for qubit-qudit states

It is now shown that the IE of Eq. (5) in the main text reduces to the I-tangle defined in [44, 45] when one considers qubit-qudit states. In particular, for two-qubit states, the IE becomes the standard tangle (squared concurrence) [41].

Consider the IE for pure states $|\psi\rangle_{AB}$ and set $H_A^\Gamma = \vec{n} \cdot \vec{\sigma}$ for some unit vector \vec{n} and the Pauli vector $\vec{\sigma}$, which is the most general way to write a qubit Hamiltonian with spectrum Γ equal to $\{-1, 1\}$. We then have that

$$\begin{aligned} \mathcal{E}^\Gamma(|\psi\rangle_{AB}) &= \min_{H_A^\Gamma} \mathcal{V}(|\psi_{AB}\rangle, H_A^\Gamma) \\ &= \min_{H_A^\Gamma} \left[\langle \psi_{AB} | (H_A^\Gamma)^2 \otimes \mathbb{I}_B | \psi_{AB} \rangle - \langle \psi_{AB} | H_A^\Gamma \otimes \mathbb{I}_B | \psi_{AB} \rangle^2 \right] \\ &= \min_{H_A^\Gamma} \left[1 - \langle \psi_{AB} | H_A^\Gamma \otimes \mathbb{I}_B | \psi_{AB} \rangle^2 \right] \\ &= 1 - \max_{H_A^\Gamma} \langle \psi_{AB} | H_A^\Gamma \otimes \mathbb{I}_B | \psi_{AB} \rangle^2 \\ &= 1 - \max_i \mu_i, \end{aligned} \quad (\text{D1})$$

where in the third equality we use the fact that $(H_A^\Gamma)^2 = (\vec{n} \cdot \vec{\sigma}_A)^2 = \mathbb{I}_A$ and in the fifth equality we set μ_i to be the eigenvalues of $\vec{r}\vec{r}^T$, with $\vec{r} = \langle \psi_{AB} | \vec{\sigma}_A \otimes \mathbb{I}_B | \psi_{AB} \rangle$ the local Pauli vector of $|\psi\rangle_{AB}$ on A . For any vector \vec{v} of unit norm, $\vec{v} \cdot \vec{r}\vec{r}^T \cdot \vec{v} = (\vec{v} \cdot \vec{r})^2 \leq \|\vec{r}\|^2$, where the equality can be saturated by choosing \vec{v} parallel to \vec{r} . Hence $\mu_{\max} \equiv \max_i \mu_i = \|\vec{r}\|^2$ so that $\mathcal{E}^\Gamma(|\psi\rangle_{AB}) = 1 - \|\vec{r}\|^2$.

Furthermore, it can be shown that

$$\frac{1 + \|\vec{r}\|^2}{2} = \text{Tr}(\rho_A^2), \quad (\text{D2})$$

with $\rho_A = \text{Tr}_B(|\psi\rangle \langle \psi|_{AB})$ the local state of subsystem A . Overall, we then have

$$\mathcal{E}^\Gamma(|\psi\rangle_{AB}) = 2(1 - \text{Tr}(\rho_A^2)), \quad (\text{D3})$$

which is (two times) the local linear entropy of $|\psi\rangle_{AB}$. The I-tangle of [44, 45] is defined for pure states as two times the local linear entropy, and for mixed states via the convex roof construction. Hence, it is clear that in the case of qubit-qudit systems with a fixed spectrum $\{-1, 1\}$, the IE is identical to

the I-tangle. For two-qubit systems, the I-tangle is equal to the standard tangle [41, 45].

$$\mathcal{T}(\rho_{AB}) = \max\{0, \lambda_1 - \lambda_2 - \lambda_3 - \lambda_4\}^2, \quad (\text{D4})$$

where $\{\lambda_i\}$ are the eigenvalues of $\sqrt{\sqrt{\rho_{AB}}\tilde{\rho}_{AB}\sqrt{\rho_{AB}}}$ in non-increasing order, with $\tilde{\rho}_{AB} = (\sigma_y \otimes \sigma_y)\rho_{AB}^T(\sigma_y \otimes \sigma_y)$ and σ_y the second Pauli matrix.

Appendix E: NMR experimental details

The two-qubit system was associated to the ^1H and ^{13}C nuclear spins contained in a Carbon-13 enriched Chloroform sample (CHCl_3). This sample was prepared by mixing 100 mg of 99% ^{13}C -labelled CHCl_3 in 0.7 mL of 99.8% CDCl_3 (both compounds provided by the Cambridge Isotope Laboratories Inc.). The experiments were performed at room temperature (around 25°C) in a BRUKER Ascend 600 MHz spectrometer located at Brazilian Agricultural Research Corporation (EMBRAPA Instrumentation, São Carlos - SP, Brazil). The spectrometer was equipped with a 5 mm double resonance probe-head with field gradient coils. In CHCl_3 , ^1H and ^{13}C are subjected to a small scalar spin-spin coupling of $J \approx 215$ Hz.

The thermal configuration of a NMR system is given by the density operator, $\rho_{eq} = \frac{1}{4}(\mathbb{I}_{AB} + \epsilon \sigma_z \otimes \sigma_z)$, where $\epsilon = \hbar\omega_L/4k_B T \sim 10^{-5}$. The deviation matrix $\Delta\rho_{eq} = \frac{1}{4}\sigma_z \otimes \sigma_z$ is the term of interest, as all the unitary transformations affect only this part. To prepare the state described in Eq. (10), first a $|00\rangle\langle 00|$ pseudopure state was prepared applying the pulse sequence $\rho_{00} - [\frac{\pi}{3}]_x^C \rightarrow G_z(\tau) \rightarrow [\frac{\pi}{4}]_x^H \rightarrow U[\frac{1}{2J}] \rightarrow [\frac{\pi}{4}]_{-y}^H \rightarrow G_z(\tau)$ to the thermal equilibrium state [66]. Here $G_z(\tau)$ corresponds to a gradient pulse applied for enough time to eliminate off-diagonal terms of the density matrix and $U(1/2J)$ represents a free evolution under J coupling for a period of $1/2J$ seconds. This step is followed by a pulse sequence where each combination of θ_1 and θ_2 (described in Table I) provides one of the experimental points in Fig. 1. HADAMARD and CNOT gates are implemented as described in the main text, as is the quantum state tomography procedure.

The error bars were estimated simulating the state preparation considering that each pulse was affected by an aleatory error, which was evaluated by pulse width (smaller than 3% for all pulses). The simulation was repeated 100 times and the error given by the distance between the theoretical state and the mean value of the error affected states.